Journal of Materials Chemistry B

Accepted Manuscript

ROYAL SOCIETY OF CHEMISTRY

www.rsc.org/materialsB

Journal of Materials Chemistry B RSCPublishing

Paper

Electro-stimulated release from a reduced graphene oxide composite hydrogel

Cite this: DOI: 10.1039/x0xx00000x

Nicky Mac Kenna,[a] Paul Calvert,[b] Aoife Morrin,[a] Gordon G. Wallace,[c] and Simon E. Moulton[c,d]

Received 00th January 2015,
Accepted 00th January 2015

DOI: 10.1039/x0xx00000x

www.rsc.org/

Electro-stimulated release was established using a novel, electro-conductive hydrogel system comprising Jeffamine polytheramine and polyethylene glycol diglycidyl ether (PEGDGE) that was composited with reduced graphene oxide (rGO). The swelling response, morphology, mechanical and electrochemical properties of the composite hydrogel were investigated. Enhanced mechanical and electrical properties were observed with increased rGO content. Passive and electro-stimulated release of methyl orange (MO) from these gels was examined. A significant reduction in passive release of the dye was observed by incorporating rGO. Upon electrical stimulation, the release rate and dosage could be tuned through variation of the % w/w rGO, as well as the polarity and amplitude of the applied electric potential. A high level of control and flexibility was achieved demonstrating the applicability of this system for localised drug delivery applications.

1. Introduction

Intelligent drug carriers capable of on-demand drug delivery are highly desirable. Traditional routes of drug administration, including oral and injection methods, commonly supply a maximum dose of drug initially which rapidly decreases over time. Alternatively, controlled drug release would provide safer, more efficient drug distribution by enabling site-specific drug delivery with on-off regulation in real time. Adverse side-effects would be dramatically reduced and patient compliance would increase. This precision could result in improved medical treatment of illnesses such as diabetes as well as personalised treatment plans for individual patients.

Considerable interest has emerged in the area of smart drug carriers such as hydrogels, liposomes, fibres and microspheres which respond to external stimuli or changes in their microenvironment e.g. pH, temperature, light, magnetic or electric fields [1-3]. Due to their high water content and unique swelling properties, hydrogels are soft, pliable materials with excellent biocompatibility. They possess many biological traits resembling natural living tissue both compositionally and mechanically[4] and their three-dimensional structure allows immobilisation of protein, peptide and DNA-based drugs. Hydrogels can be injected or implanted at the target site, creating localised drug delivery while their viscoelastic nature minimises damage to the host [5, 6]. Once implanted the hydrogel can swell or biodegrade to release the drug. If cell microencapsulation techniques are utilised the active drug component can be protected from triggering an immune response [7].

Various external stimuli have been employed recently to initiate drug release from smart materials *in vivo*. These include use of ultrasound, radiofrequency, light, NIR and laser radiation, magnetic and electric fields [8, 9]. Use of an electric field as an applied stimulus has many advantages, including reliability and precise control of magnitude, duration and intervals of pulses. The application or removal of an electrical field can trigger drug release similar to the pulsatile release of numerous endogenous chemicals *in vivo* including insulin, oestrogen and growth hormones. Electric fields can be generated by applying an electro-conducting patch to the skin above the implanted gel. Electrodes are then connected to the patch and the electric field is switched on. Iontophoresis and electroporation have been utilised for drug delivery *in vivo* [3, 10, 11].

However, many hydrogels are inherently non-conductive and require the addition of an electroactive component. These electroconductive hydrogels (ECHs) can be prepared by producing the gel directly from conducting polymers [12, 13], incorporating inherently conducting polymers (ICPs) [14, 15] or conductive particles into the hydrogel network [16-18]. When composited together, these materials aim to integrate the unique properties of their constituents, i.e., the high water content, biocompatibility and 3D matrix of hydrogels with the electrical conductivity and switchable electrical and optical properties of the selected conductive materials. Use of carbon nanomaterials, such as carbon nanotubes (CNTs), graphene, graphene oxide (GO) and rGO, can attribute a large surface area, high electrical conductivity and enhanced mechanical properties. These properties facilitate a high drug loading, while the sp^2 carbon lattice and active oxygen-containing functional groups of for example, rGO enable modification and functionalization opportunities for targeted and controlled drug delivery.

Electro-stimulated release from CNTs in a chitosan hydrogel was achieved by Naficy *et al.* [19]. They demonstrated good potential for a controlled release platform based on

electrostatic interactions between CNTs and dexamethasone. It has been reported that graphene materials have a larger surface area than CNTs due to their planar structure [20]. This suggests that higher charge could be generated by incorporating graphene materials, leading to faster and possibly higher drug release. Also, passive release could potentially be reduced by additional positive charge and a higher capacity for adsorption. Liu *et al*. [21] investigated electro-modulated release of lidocaine hydrochloride from rGO in a poly(vinyl) alcohol (PVA) hydrogel. On demand drug release was feasible with release profiles varying from slow elution to rapid release. However, large voltages were required which may not be permitted *in vivo*.

This work describes the synthesis and characterisation of an electroactive hydrogel composite and its potential application in electro-stimulated drug delivery. A high loading of rGO (20% w/w) was incorporated into a Jeffamine-PEGDGE hydrogel in a single polymerisation step. For drug delivery experiments, methyl orange (MO) was added as a model drug. MO is negatively charged and can be expelled/retained according to the applied electrical stimulus. This is attributed to electrostatic interactions between the rGO and MO during charging. The high surface area of rGO permitted use of low applied potentials for electro-stimulation. By selection of the rGO loading, polarity and amplitude of the applied potential electro-modulation of the release profile was achieved.

2. Experimental

2.1 Materials

Jeffamine® EDR-148 polyetheramine was donated by Huntsman Chemical Company (US). Poly (ethylene glycol) diglycidyl ether (PEGDGE, Average Mn 526), hyaluronic acid potassium salt from human umbilical cord and phosphate buffered saline (PBS) tablets pH 7.4 were purchased from Sigma-Aldrich. The Intelligent Polymer Research Institute (Wollongong, Australia) prepared and supplied the reduced graphene oxide using natural graphite powder purchased from Bay Carbon (US). Untreated carbon cloth (44 x 48 yarns/inch, 99% carbon) was purchased from Fuel Cell Store (US). Potassium ferricyanide was obtained from Univar (Australia). Silver/silver chloride (Ag/AgCl) electrodes and platinum mesh were purchased from IJ Cambria Scientific Ltd (UK) and Sigma-Aldrich (Ireland) respectively.

2.2 rGO hydrogel synthesis

The production and characterisation of the rGO has been reported by Gambhir et al. [22]. In brief, graphene oxide (GO) was prepared by oxidation/exfoliation of natural graphite powder via a modified Hummer's method. The GO was subsequently reduced to rGO with hydrazine, acidified to pH <2 using dilute sulphuric acid, thoroughly washed and dried under vacuum to produce rGO powder.

An aqueous dispersion of rGO (2 mg/mL) was prepared using hyaluronic acid (0.03%) as a dispersing agent. The dispersion remained highly stable after ultrasonication using a Branson Digital Sonifier at 35 % amplitude for 2 hr (4 s on and 2 s off pulses) with continuous cooling in an ice bath. Small aliquots were collected regularly and dropped on a glass slide to assess the dispersion quality under a light microscope. A cover slip was placed on top to prevent drying and ensure appropriate viewing thickness.

Various amounts of the rGO dispersion (0.5% - 20% w/w) were incorporated into a 1:1 molar ratio solution of Jeffamine® EDR-148 polyetheramine and PEGDGE in DI water with vortexing (Schematic – Fig. 1). All hydrogels were polymerised in the refrigerator (4°C) overnight to reduce evaporation. The Jeffamine-PEGDGE hydrogels containing rGO will be referred to as "rGO-hydrogel" and without the rGO simply "hydrogel" from here on in the manuscript.

2.3 Characterisation

The swelling behaviour of the rGO hydrogel was determined gravimetrically. 4 g of each hydrogel monomer mixture was poured into a small petri-dish (53 mm internal diameter) and placed in the refrigerator (4°C) overnight to cure. Cylindrical gel discs (5 mm diameter and 0.8 mm thick) were cut from the polymerised hydrogel membrane. Each disc was weighed (W_{dry}) before immersion into DI water. At specific time intervals, the swollen discs were removed from solution, blotted dry with filter paper and re-weighed (W_{wet}). The swelling ratio at various time intervals was calculated using equation 1:

$$\text{Swelling ratio} = \frac{W_{wet} - W_{dry}}{W_{dry}} \quad (1)$$

SEM micrographs were obtained using a Jeol JSM-6490LA scanning electron microscope at an accelerating voltage of 15 kV. Equilibrium water-swollen hydrogels were flash frozen in liquid nitrogen (for 45 s) on a brass plate and cryofractured using a scalpel blade to obtain cross-sections of the internal structure.

Uniaxial compression measurements were performed using a universal testing machine (EZ-L Shimadzu) fitted with a 10 N load cell. Equilibrium water-swollen hydrogels (5.5 mm width, 15 mm in diameter) were compressed at a strain rate of 2 mm/min until fracture. Force and displacement data were recorded with Trapezium X software and converted into stress-strain curves for analysis.

All electrochemical characterisation was performed in PBS (10 mM; pH 7.4) on a CHI660C or CHI660D electrochemical analyser, using cyclic voltammetry or AC impedance modes. A three electrode system was utilised with a hydrogel-modified carbon cloth working electrode, platinum mesh auxiliary electrode and Ag/AgCl reference electrode. Hydrogel-modified carbon cloth electrodes were prepared by cutting segments (4 cm x 1 cm) from a large sheet of carbon cloth. The working electrode area (0.5 cm x 0.5 cm) was defined using insulating varnish and, once dried, dip-coated into a solution of the hydrogel precursors to apply the hydrogel. Electrodes were

swollen for 24 hr in solution before electrochemical measurements were taken.

Cyclic voltammograms were obtained by cycling carbon cloth electrodes between -0.2 V and 0.7 V (without ferricyanide present in the PBS) or -0.1 V and 0.5 V (with 2 mM ferricyanide present in the PBS) vs. Ag/AgCl at a scan rate of 50 mV s^{-1}. Electrochemical impedance spectra were collected at the open circuit potential (OCP), in a frequency range of 0.1 to 10000 Hz, with an alternating current sinusoid of ± 10 mV amplitude.

2.4 Model Drug (MO) Release

Hydrogel-modified carbon cloth electrodes were prepared with dip-coats of 0% w/w, 5% w/w and 20% w/w rGO-hydrogels containing 0.654% w/w dissolved methyl orange (MO). PBS (10 mM; pH 7.4) at room temperature (ca. 22 °C) was used as the release media for all release experiments. For passive release, electrodes were placed in PBS (1.5 mL) and moved to fresh PBS solutions at selected time points. For electrically stimulated release, the three electrode configuration was used and the release media (8 mL) was gently stirred. Constant potentials of -0.6 V, -0.2 V and 0.6 V (vs. Ag/AgCl) were applied to the dye loaded hydrogel system. At specific time intervals, 1 mL aliquots of the release media were collected and replenished with 1 mL of fresh PBS. MO release was quantified by measuring the absorbance of the aliquots at 493 nm using a Shimadzu 1800 UV-vis spectrophotometer. Dilution factors and swelling volumes were considered in the release calculations. A release profile was generated by plotting the cumulative methyl orange release as a percentage of the initial amount incorporated.

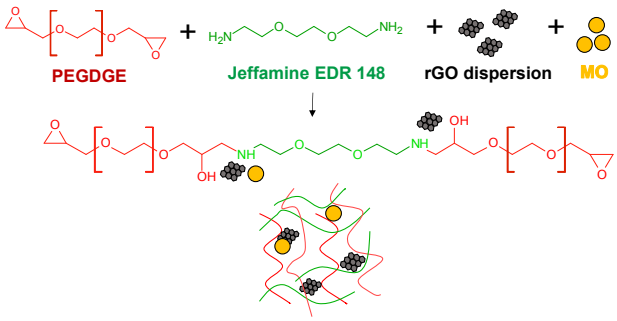

Fig. 1 Schematic of rGO-hydrogel formation for MO release.

3. Results & Discussion

3.1 Incorporation of rGO into hydrogels

Hydrogel formation can be a slow process when cross-linking occurs spontaneously (i.e., without use of heat or UV light) such as the hydrogel system described here. Consequently, the rGO solution must be highly stable and remain homogenously dispersed throughout the hydrogel monomer mixture to ensure good distribution of rGO throughout the formed hydrogel network. This is paramount for creating interconnected electrical pathways and increasing the overall conductivity of the gel. To achieve a stable rGO dispersion, hyaluronic acid (HA) was utilised as a dispersing agent since HA has been shown to act as an effective dispersing agent for rGO nanosheets and carbon nanotubes[23-26]. Additionally, as a major component of the extracellular matrix, HA is highly biocompatible and contributes to tissue repair by cell proliferation, migration and moderation of the inflammatory response[27, 28]. Only a very small amount of HA (0.03% w/w) was required to obtain a rGO dispersion (at a rGO concentration of 2 mg/mL) which was stable for more than 6 months. The presence of the HA did not hinder the crosslinking process and enabled a high loading capacity of rGO (up to 20% w/w) into the hydrogels. Fig. 2 show the hydrogels prepared from rGO dispersions with and without HA. It can clearly be seen that without the dispersing agent HA the rGO agglomerates. This is particularly visible in the 0.5% rGO-No HA sample in Fig. 2. The aggregation present in the 5% and 20% rGO-No HA hydrogels is not as visible due to their high concentration of rGO. Hydrogels prepared using the HA dispersed rGO appear homogeneous, even at the highest rGO loading of 20%.

All rGO-hydrogels retained the rGO in the network even when fully swollen and at prolonged immersion times (longer than 4 days) suggesting strong interactions between the rGO and the Jeffamine-PEGDGE backbone. It is postulated that strong hydrogen bonds form between the -OH and –COOH groups of rGO and the –OH and $–NH_2$ groups of the Jeffamine-PEGDGE backbone. X-ray diffraction studies and x-ray photoelectron spectroscopy were performed previously to confirm the presence of these oxygen-containing groups on the rGO after its reduction from GO[22].

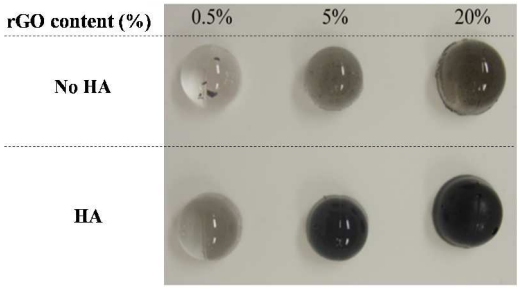

Fig. 2 Hydrogels with various rGO loadings without a dispersing agent (No HA) and using HA as the dispersing agent (HA).

3.2 Swelling response

The swelling response of rGO-hydrogel discs with rGO loadings from 0.5 - 20% w/w was investigated. Fig. 3 displays the swelling behaviour of these rGO-hydrogels and hydrogel in DI water at room temperature. It is clear that all samples swell rapidly initially and the swelling rate decreases over time. The rGO content had negligible impact on the time required to reach swelling equilibrium (~ 45 hr). As mentioned above no leeching of rGO from the rGO-hydrogel samples into the solution was observed. The equilibrium swelling ratio

decreased gradually with increasing rGO content. This is attributed to negatively charged rGO possibly associating with the positive charge on the Jeffamine and imparting an ionic crosslinking effect which in turn increases the cross-linking density of the network and the possible formation of defects in the network structure such as meshes and grafts. It is well known that the swelling response of a hydrogel is heavily dependent on its cross-linking density. Additional cross-links and structural defects reduce the swelling capacity of the hydrogels decreasing water uptake and swelling ratios.

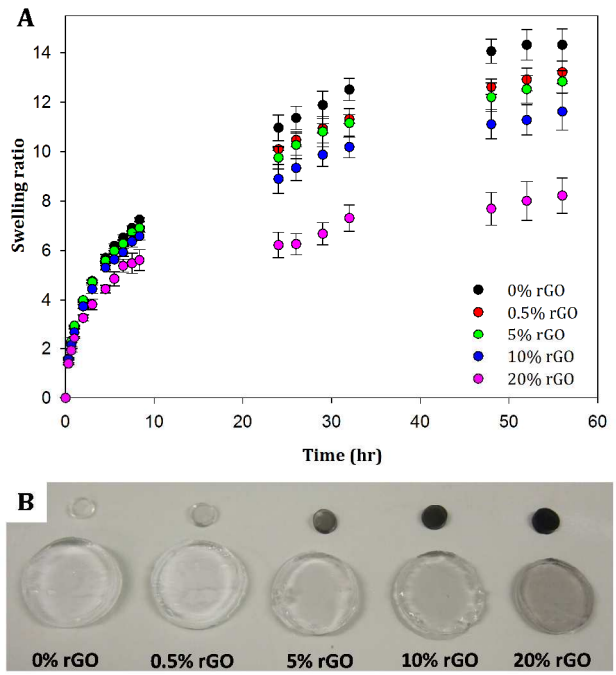

Fig. 3 Swelling response of rGO-hydrogels and hydrogel (0% rGO) in DI water at room temperature (A). Images (B) of the samples prior to immersion into DI water (top) and after equilibration in deionised water at room temperature (bottom).

3.3 SEM analysis

The morphology of the rGO-hydrogels was investigated using low vacuum SEM (Fig. 4). SEM images of fully swollen rGO-hydrogel containing 20% rGO were recorded and compared with hydrogel containing no rGO. All samples were flash-frozen in liquid nitrogen for 45 s and fractured to view their internal structure. A smooth sponge-like architecture, with a wide pore size distribution, was observed for all samples with the presence of rGO (Fig. 4A) indistinguishable from the hydrogel network. There were no apparent structural differences in the rGO-hydrogels which could be attributed to the rGO. This indicates that the rGO does not have a significant impact on the morphology of the hydrogels.

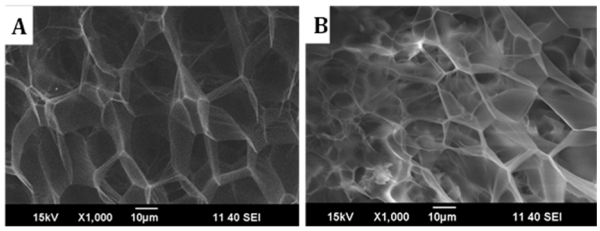

Fig. 4 SEM images of a (A) rGO-hydrogel containing 20% rGO hydrogel and a hydrogel containing no rGO (B).

3.4 Mechanical properties

Typical stress-stain curves of the rGO-hydrogels under compression are shown in Fig. 5 with the calculated mechanical properties presented in Table 1. All hydrogels displayed non-linear hyperelastic stress-strain curves, similar to biological soft tissue. Higher stress and compressive moduli were sustained as the rGO loading in the hydrogels was increased. In comparison with the unmodified hydrogel (18.9 ± 7.0 kPa), 5% rGO hydrogels had compressive strengths of 30.6 ± 7.4 kPa and 20% rGO gels had compressive strengths of 51.2 ± 7.7 kPa, increasing by 62% and 171% respectively. Additionally, the modulus increased by 136% with the addition of 20% rGO to the hydrogel (1.9 ± 0.7 kPa to 4.5 ± 0.4 kPa). These results indicate that incorporation of rGO reinforces the hydrogel network and improves load transfer between the network and the rGO sheets, enhancing the mechanical properties. A similar behaviour has been seen previously with incorporation of graphene oxide into poly(vinyl) alcohol (PVA) and poly(acrylic) acid (PAA) based hydrogels [29-32].

However, while the mechanical properties of the unmodified hydrogels improve when composited with rGO, they may still be regarded as relatively weak in comparison with other hydrogel systems. This is predominately because these hydrogels have been prepared with a 1:1 Jeffamine:PEGDGE ratio, resulting in a low cross-linking density in the polymer matrix. This design choice yields high swelling ratios, whilst compromising on mechanical strength[33]. High swelling ratios can be advantageous for drug delivery applications as faster release rates can be achieved or higher dosages released.

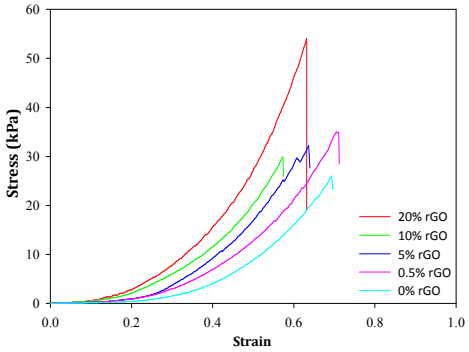

Fig. 5 Typical stress-strain curves for rGO hydrogels. Testing was performed in compressive mode using 10 N load cell at a strain rate of 2 mm/min until fracture.

Table 1. Mechanical (compression) properties of hydrogels with and without the inclusion of rGO.

Sample	Initial Modulus (kPa)	Modulus before break (kPa)	Breaking Strain (%)	Breaking Stress (kPa)
0% rGO	1.9 ± 0.7	104.1 ± 1.8	61.7 ± 6.8	18.9 ± 7.0
0.5% rGO	2.2 ± 0.4	119.4 ± 28.2	63.9 ± 7.4	28.2 ± 4.9
5% rGO	2.8 ± 0.5	125.9 ± 36.4	61.1 ± 8.6	30.6 ± 7.4
10% rGO	3.7 ± 0.7	159.8 ± 21.2	56.2 ± 2.3	32.3 ± 5.2
20% rGO	4.5 ± 0.4	244.9 ± 19.0	62.1 ± 6.5	51.2 ± 7.7

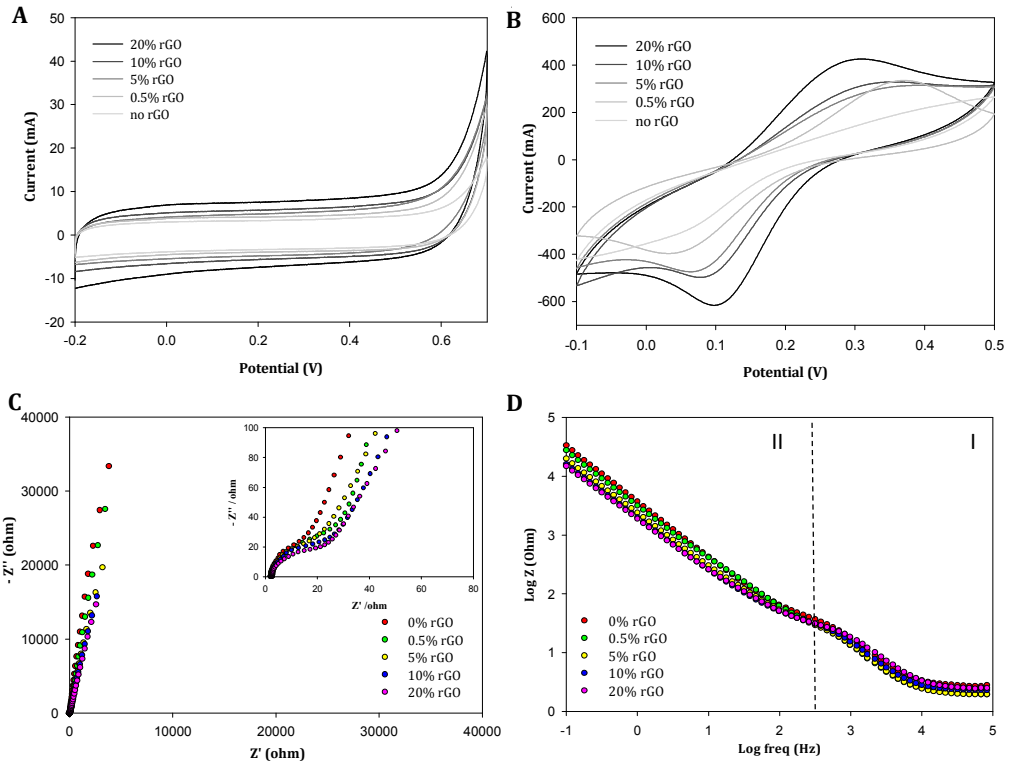

Fig. 6 Cyclic voltammograms of the hydrogel (0% rGO) and rGO-hydrogels with increasing rGO content recorded in PBS (10mM; pH 7.4) (A) and in 2 mM ferricyanide (in PBS 10mM; pH 7.4) (B) at a scan rate of 50 mV s^{-1}. Nyquist (C) and Bode (D) plots for all hydrogel samples recorded in 10 mM PBS; pH 7.4. EIS was measured at the rGO-hydrogels open circuit potential between 0.1 and 10000Hz.

3.5 Electrochemical behaviour

The electrochemical properties of the rGO-hydrogels were evaluated using cyclic voltammetry (CV) and electrochemical impedance spectroscopy (EIS). In order to characterise the capacitance properties and electron transfer properties, voltammetry was assessed both in PBS (10 mM, pH 7.4) and in the presence of the ferri/ferrocyanide redox couple, respectively. Higher currents and increased capacitance was observed as the rGO content increased (Fig. 6A) corresponding to the rGO providing a larger electroactive surface area. A close to ideal non-Faradaic voltammogram was observed when increasing the potential scan rate from 1 – 200 mV/s (data not shown), indicating excellent charge propagation and ionic transport within the rGO-hydrogels. Additionally, Fig. 6B depicts the peak current (ip) values increasing and the bulk solution Fe^{2+}/Fe^{3+} and an observed decrease in the peak-to-peak separation for the oxidation and reduction processes indicating improved redox switching with increasing rGO content. For example, the ip for the redox couple increased by approximately 43% and the ΔEp value reduced from 0.339 V to 0.205 V when the rGO content in the hydrogel was increased from 0.5% to 20%. It is apparent that the rGO is lowering the electric resistance and enhancing the charge transfer properties.

Complementary to the voltammetry results, a similar trend was detected using EIS (Fig. 6C and D). The EIS spectra (Fig. 6C) comprise a high frequency intercept on the real Z' axis and the beginning of a semi-circular arc across the high to low frequency range. The high frequency intercept is representative of a combination of electrolyte ionic resistance, the intrinsic resistance of the carbon cloth and the resistance of the contacts to the potentiostat. The semi-circular arc, is representative of the capacitive and resistive behaviour of the rGO-hydrogels with the resistance observed to decrease with increasing rGO content.

The Bode plot (Fig. 6D) can be divided into two frequency regions indicative of the dominant kinetics within each domain. The domain above 400 Hz shows resistive behaviour (I), while the domain from 400 Hz to 0.1 Hz shows the capacitance behaviour of the rGO-hydrogel is dominant (II). Maximum changes in the magnitude of log Z were seen within this region with the hydrogels with a higher rGO content observed to have lower impedance. This decrease in impedance is attributed to

the increase in the electrically connected network as the percentage of rGO increases.

3.6 Methyl orange release

3.6.1 Passive release

Methyl orange (MO), an anionic dye (Fig. 7 insert) with a low molecular weight, was selected as the model drug for evaluating the release behaviour of the rGO-hydrogels. Passive release was investigated from rGO-hydrogels containing 5% and 20% rGO, representing a 'low' and 'high' amount of rGO, and compared against the unmodified Jeffamine-PEGDGE hydrogel. The cumulative release profile over 4380 min (~ 3 days) in PBS (10 mM, pH 7.4) at room temperature is shown in Fig. 7. Rapid release of MO was observed for the first 180 min with approximately 70% of the MO being released from the unmodified hydrogel (0% rGO). A significant reduction in the release rate occurred subsequently, with the remaining 30% MO requiring 4200 min to be fully released. Since no stimulation was applied to the samples the release rate was governed by passive diffusion of the MO from the hydrogel into the release medium. The initial rapid release occurs from MO located near the surface or loosely bound within the gel. The diffusion path length is much longer for MO molecules located deeper within the hydrogel network leading to prolonged release.

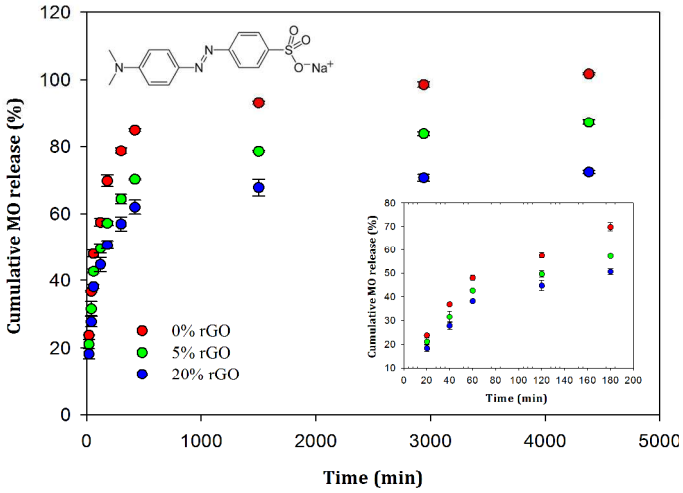

Fig. 7 Passive release into PBS (10 mM, pH 7.4) at room temperature of MO from rGO-hydrogels (Inset: Early passive release time points). All samples were loaded with the same amount of MO. The chemical structure of MO is shown.

Lower passive release profiles were observed for the rGO-hydrogels with 87% and 72% total cumulative release being obtained for the 5% w/w and 20% w/w rGO-hydrogels respectively. The inclusion of rGO also resulted in observed slower release rates. After 180 min only 57% and 50% of MO was released from the 20% w/w and 5% w/w samples respectively, compared to 70% for the hydrogel containing no rGO. Previous studies have shown that drug release from hydrogels closely follows the extent of hydrogel swelling, namely the greater the swelling the greater the release [34-36]. This is also the case for our hydrogels (Fig. 3 and 7 respectively) indicating that for passive release the presence of the rGO does not hinder this diffusion process during swelling. Also, the amount released is possibly reduced by MO adsorption onto the rGO sheets as many carbonaceous materials, including graphene, GO and CNTs, display high binding affinities for dyes such as MO [37-40]. Previous work has indicated that this property arises from π-π stacking interactions, oxygen-containing functional groups [40], electrostatic attraction and high specific surface areas [41]. In drug delivery applications, reduced passive diffusion may be highly desirable for administering accurate doses efficiently and minimising potential side-effects.

3.6.3 Electro-stimulated release

The electro-stimulated release experiments investigated the influence of rGO content, as well as the polarity and amplitude of the applied electric potential on the release characteristics of the MO. The mechanism for this release system is based on electrostatic repulsion between the anionic dye and the rGO during charging. It would be expected that negative potentials would trigger electrostatic repulsion between MO and rGO, accelerating release, whilst positive potentials would induce electrostatic attraction, thereby retarding or suspending the release. In addition to field effects, it is possible that there is also capacitive deionisation associated with the applied voltages contributing to the release. The MO containing rGO-hydrogel samples were prepared using the same methodology described previously for preparing the samples for electrochemical characterisation. The MO was incorporated into the rGO-hydrogel as described above with the release experiments being performed in PBS (10 mM, pH 7.4) at room temperature. A release duration of 180 min was selected as this is where the majority of the release occurred in the passive experiments detailed above. Applied voltages of +0.6 V, -0.2 V and -0.6 V were chosen as the rGO-hydrogels demonstrated excellent charging behaviour in this range during the voltammetry studies (Fig. 6). The cumulative MO release from hydrogels containing no rGO under electrostimulation (see Electronic Supplementary Information), did not show any variation from the passive release shown for the first 180 min in Fig. 7. This was anticipated as there is no conductive moiety incorporated into these hydrogels. Application of a dc field can sometimes induce swelling in polyelectrolyte hydrogels, such as these, which could influence drug release but this was not seen in our system as much larger potentials are generally required (~6 V) [33]. Such high potentials may not be permitted *in vivo* and previous studies have shown that GO may be reversibly oxidised and reduced using electrical stimulation of 2-3 V [42] which would be highly unfavourable for this system.

Fig. 8A and 7B show the passive and stimulated release profiles for 20% w/w and 5% w/w rGO-hydrogels respectively. The release rate and amount can be modulated by altering the polarity and amplitude of the applied potential, as well as the percent loading of rGO. In terms of electrode polarity, accelerated release was observed upon application of a negative potential. Alternatively when a positive potential is applied the

extent of release decreased below that of passive release. These trends were observed for both the 5% w/w and 20% w/w rGO-hydrogels. After 180 min, 50% release was recorded under passive conditions for the 20% w/w rGO-hydrogel compared to 76% release when a voltage of -0.6 V was applied and this decreased to 24% when +0.6 V is applied. This broad range offers significant control of the release quantity over a narrow time period.

Furthermore, the amplitude of the applied stimulus influenced the release profile. Higher release was achieved for rGO-hydrogels at -0.6 V compared to -0.2 V. The 20% rGO-hydrogels released 64% of their MO content at -0.2 V versus 76% at -0.6 V after 3 hr. This is attributed to the generation of a higher charge density at more negative voltages, thus increasing the electrostatic repulsion between MO and rGO, leading to an accelerated release. The same trends are visible for 5% rGO-hydrogels in Fig. 8B.

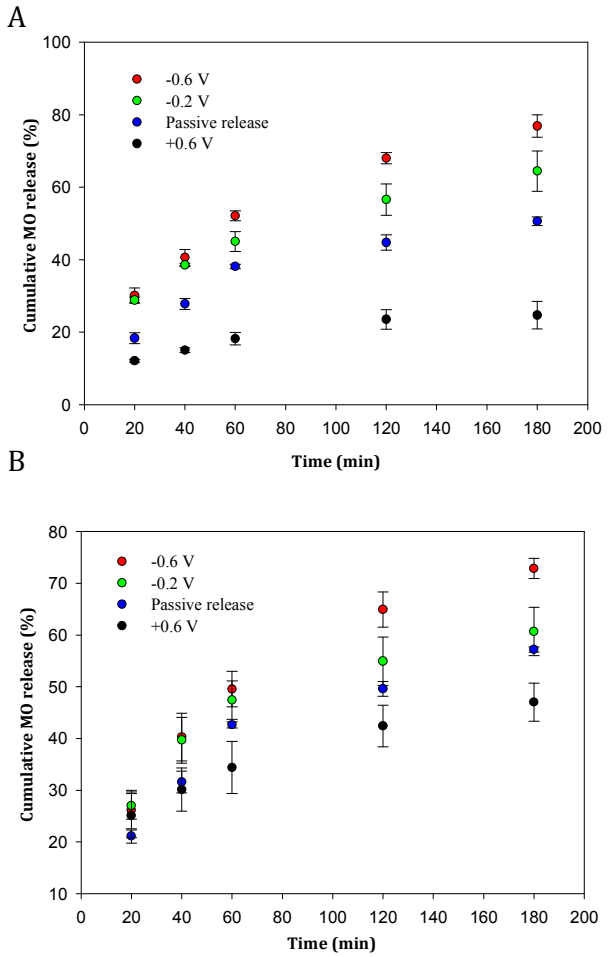

Fig. 8 Cumulative MO release from (A) 20% rGO- and (B) 5% rGO-hydrogels under passive and electro-stimulated conditions.

A wider range in the amount of MO released was observed for 20% rGO-hydrogels compared to 5% rGO-hydrogels. This corresponds with the increase in capacitance observed with rGO content in the voltammetry and EIS studies (Fig. 6). The hydrogels with a higher loading of rGO expel greater amounts of MO at applied negative potentials and lower amounts at positive potentials than hydrogels with low rGO content, corresponding to an increase in electrical conductor density. As previously stated, release from hydrogels is highly dependent on the extent of swelling, however for the rGO-hydrogels developed in this work, the results from Fig. 8 clearly demonstrate that release can be modulated by the application of an applied voltage. These results strongly indicate that under appropriate electro-stimulated conditions the release is primarily dominated by electrical behaviour of the hydrogels and not the swelling properties.

4. Conclusions

A novel electroconductive hydrogel capable of electro-stimulated release has been developed. Incorporation of very low concentrations of HA greatly improved the stability of rGO dispersions and allowed the production of high quality, homogeneous rGO-hydrogel composites. The inclusion of rGO attributed new properties and enhanced the inherent characteristics of a Jeffamine-PEGDGE hydrogel system. Increased mechanical strength and electrochemical properties were also demonstrated. On-demand controlled release was achieved with these new composite materials. Through variation of the rGO content, electrode polarity and magnitude, a wide number of release profiles were observed, ranging from slow release of low concentrations to rapid release of high concentrations. The effects of ionic strength, as well as the cytotoxicity of the hydrogel and precursors, are yet to be evaluated. This versatile delivery platform has demonstrated great potential towards advancing current delivery systems by exhibiting great control and precision over tuneable release profiles.

Acknowledgements

The authors gratefully acknowledge financial assistance from FP7-PEOPLE-2010-IRSES GA 269302, the Irish Research Council for the EMBARK initiative scholarship (NMK) and the Walton Fellowship (PC). The authors also thank the Australian Research Council (ARC) for continuing financial support (CE 140100012). GGW grateful to the ARC for support under the Australian Laureate Fellowship scheme (FL110100196). The authors also acknowledge use of the Australian National Fabrication Facility (ANNF) Materials Node, in particular Dr Sanjeev Gambhir, for the supply of the rGO. The authors also acknowledge use of the facilities and the assistance of Mr. Tony Romeo at the UOW Electron Microscopy Centre.

Notes and references

[a] National Centre for Sensor Research, Dublin City University, Dublin 9, Ireland.
[b] Bioengineering, University of Massachusetts Dartmouth, Dartmouth, USA.
[c] ARC Centre of Excellence for Electromaterials Science, Intelligent Polymer Research Institute, University of Wollongong, Wollongong, NSW 2522, Australia.

[d] Biomedical Engineering, Faculty of Science, Engineering and Technology, Swinburne University of Technology, Hawthorn, Vic, 3122, Australia. E-mail: smoulton@swin.edu.au

Electronic Supplementary Information (ESI) available: [details of any supplementary information available should be included here]. See DOI: 10.1039/b000000x/

1. S. E. Moulton and G. G. Wallace, Journal of Controlled Release, 2014, DOI: http://dx.doi.org/10.1016/j.jconrel.2014.07.005.
2. Y. Qiu and K. Park, Advanced Drug Delivery Reviews, 2001, 53, 321-339.
3. S. Murdan, Journal of Controlled Release, 2003, 92, 1-17.
4. M. Sirousazar and M. Kokabi, Intelligent Nanomaterials, Scrivener Publishing LLC, Massachusetts, 2012.
5. D. Ding, Z. Zhu, R. Li, X. Li, W. Wu, X. Jiang and B. Liu, ACS Nano, 2011, 5, 2520-2534.
6. K. H. Bae, L. S. Wang and M. Kurisawa, Journal of Materials Chemistry B, 2013, 1, 5371-5388.
7. K. Deligkaris, T. S. Tadele, W. Olthuis and A. van den Berg, Sensors and Actuators B: Chemical, 2010, 147, 765-774.
8. S. Mura, J. Nicolas and P. Couvreur, Nature Materials, 2013, 12, 991-1003.
9. D. A. LaVan, T. McGuire and R. Langer, Nature Biotechnology, 2003, 21, 1184-1191.
10. A. R. Denet, R. Vanbever and V. Preat, Advanced Drug Delivery Reviews, 2004, 56, 659-674.
11. M. B. Brown, G. P. Martin, S. A. Jones and F. K. Akomeah, Drug Delivery, 2006, 13, 175-187.
12. L. J. Pan, G. H. Yu, D. Y. Zhai, H. R. Lee, W. T. Zhao, N. Liu, H. L. Wang, B. C. K. Tee, Y. Shi, Y. Cui and Z. N. Bao, Proc. Natl. Acad. Sci. U. S. A., 2012, 109, 9287-9292.
13. Y. Shi, L. Pan, B. Liu, Y. Wang, Y. Cui, Z. Bao and G. Yu, Journal of Materials Chemistry A, 2014, 2, 6086-6091.
14. S. Naficy, J. M. Razal, G. M. Spinks, G. G. Wallace and P. G. Whitten, Chemistry of Materials, 2012, 24, 3425-3433.
15. S. Brahim and A. Guiseppi-Elie, Electroanalysis, 2005, 17, 556-570.
16. S. Ahadian, J. Ramón-Azcón, M. Estili, X. Liang, S. Ostrovidov, H. Shiku, M. Ramalingam, K. Nakajima, Y. Sakka, H. Bae, T. Matsue and A. Khademhosseini, Scientific Reports, 2014, 4.
17. T. Dvir, B. P. Timko, M. D. Brigham, S. R. Naik, S. S. Karajanagi, O. Levy, H. Jin, K. K. Parker, R. Langer and D. S. Kohane, Nature Nanotechnology, 2011, 6, 720-725.
18. N. J. Whiteside, G. G. Wallace and M. in het Panhuis, Synthetic Met, 2013, 168, 36-42.
19. S. Naficy, J. M. Razal, G. M. Spinks and G. G. Wallace, Sensors and Actuators A: Physical, 2009, 155, 120-124.
20. C. Bussy, H. Ali-Boucetta and K. Kostarelos, Accounts of Chemical Research, 2012, 46, 692-701.
21. H.-W. Liu, S.-H. Hu, Y.-W. Chen and S.-Y. Chen, Journal of Materials Chemistry, 2012, 22, 17311-17320.
22. S. Gambhir, E. Murray, S. Sayyar, G. G. Wallace and D. L. Officer, Carbon, 2014, 76, 368-377.
23. J. Filip, J. Šefčovičová, P. Tomčík, P. Gemeiner and J. Tkac, Talanta, 2011, 84, 355-361.
24. W. Miao, G. Shim and K. Choong Mo, Biomaterials, 2013, 34, 9638-9647.
25. C. Lynam, S. E. Moulton and G. G. Wallace, Advanced Materials, 2007, 19, 1244-1248.
26. J. M. Razal, K. J. Gilmore and G. G. Wallace, Adv. Funct. Mater., 2008, 18, 61-66.
27. S. E. Moulton, M. Maugey, P. Poulin and G. G. Wallace, J. Am. Chem. Soc., 2007, 129, 9452-9457.
28. D. Jiang, J. Liang and P. W. Noble, in Annual Review of Cell and Developmental Biology, Annual Reviews, Palo Alto, 2007, vol. 23, pp. 435-461.
29. Y. Xu, W. Hong, H. Bai, C. Li and G. Shi, Carbon, 2009, 47, 3538-3543.
30. L. Zhang, Z. Wang, C. Xu, Y. Li, J. Gao, W. Wang and Y. Liu, Journal of Materials Chemistry, 2011, 21, 10399-10406.
31. Y. X, T. Y, L. L, S. S and T. XM, ACS Applied Materials and Interfaces, 2010, 2, 1707-1713.
32. S. Faghihi, A. Karimi, M. Jamadi, R. Imani and R. Salarian, Materials Science and Engineering: C, 2014, 38, 299-305.
33. Y. Yoshioka and P. Calvert, Experimental Mechanics, 2002, 42, 404-408.
34. M. Amin, N. Ahmad, N. Halib and I. Ahmad, Carbohydr. Polym., 2012, 88, 465-473.
35. P. Gupta, K. Vermani and S. Garg, Drug Discovery Today, 2002, 7, 569-579.
36. H. Omidian and K. Park, Journal of Drug Delivery Science and Technology, 2008, 18, 83-93.
37. Y. J. Yao, B. He, F. F. Xu and X. F. Chen, Chem. Eng. J., 2011, 170, 82-89.
38. T. H. Tsai, S. C. Chiou and S. M. Chen, International Journal of Electrochemical Science, 2011, 6, 3333-3343.
39. J. Ma, F. Yu, L. Zhou, L. Jin, M. X. Yang, J. S. Luan, Y. H. Tang, H. B. Fan, Z. W. Yuan and J. H. Chen, ACS Appl. Mater. Interfaces, 2012, 4, 5749-5760.
40. Y. Wang, X. Liu, H. Wang, G. Xia, W. Huang and R. Song, Journal of Colloid and Interface Science, 2014, 416, 243-251.
41. Y. L. Wang, P. Gao, L. H. Huang, X. J. Wu and Y. L. Liu, Chin. J. Inorg. Chem., 2012, 28, 391-397.
42. O. Ö. Ekiz, M. Ürel, H. Güner, A. K. Mizrak and A. Dâna, ACS Nano, 2011, 5, 2475-2482.

Graphical Abstract

Composite hydrogel containing reduced graphene oxide (rGO) demonstrating the ability to perform electro-stimulated controlled release.